Analysis of the ∞-replica symmetry breaking solution of the Sherrington-Kirkpatrick model

A. Crisanti*
Dipartimento di Fisica, Università di Roma "La Sapienza," and Istituto Nazionale Fisica della Materia, Unità di Roma, Piazzale Aldo Moro 2, I-00185 Roma, Italy

T. Rizzo
Dipartimento di Scienze Fisiche, Università "Federico II," Complesso Monte S. Angelo, I-80126 Napoli, Italy
(Received 8 November 2001; published 10 April 2002)

In this work we analyze the Parisi ∞-replica symmetry breaking solution of the Sherrington-Kirkpatrick model without external field using high order perturbative expansions. The predictions are compared with those obtained from the numerical solution of the ∞-replica symmetry breaking equations, which are solved using a pseudospectral code that allows for very accurate results. With these methods we are able to get more insight into the analytical properties of the solutions. We are also able to determine numerically the end point $x_{\max}$ of the plateau of $q(x)$ and find that $\lim_{T\to 0} x_{\max}(T) > 0.5$.

DOI: 10.1103/PhysRevE.65.046137 PACS number(s): 05.50.+q, 75.10.Nr, 75.40.Cx, 02.70.Hm

I. INTRODUCTION

Since its proposal in the 1980s the behavior of the Parisi ∞-replica symmetry breaking (∞-RSB) solution of the Sherrington-Kirkpatrick (SK) model has been extensively investigated both qualitatively and quantitatively [1,2]. Despite this enormous amount of work, which has revealed many of the properties of the solutions, complete control of the solution is still missing. One of the reasons can be traced back to the fact that until now only low order expansions have been used, and moreover applied often to reduced forms of the ∞-replica symmetry breaking equations valid only near the critical temperature. From the numerical point of view there are only a few works that confirm the general properties of the solution but do not allow for high accuracy. On the other hand, ∞-replica symmetry breaking solutions of the type encountered in the SK model have been found in other models of interest in different fields, e.g., in computer science with solvability problems [3] or in the study of the structural glass transition [4–6].

Motivated by these problems, we believe that it would be quite useful to have some reliable and efficient tool to find good approximations of the full solution far from the critical points also. In this work we reconsider two approaches. The first one is based on expansions for temperatures near the critical temperature T_c. As we said above, previous work considered only low order expansions [7–9]. Here, by using algebraic manipulators, we push the expansion to rather high orders and by resumming it via the Padé resummation technique we are able to a get a good estimate of the solution for a wide range of temperature below T_c.

The second approach is numerical. Previous numerical studies of the ∞-replica symmetry breaking solution used a naive integration scheme based on the direct discretization of the Parisi equation [10–13]. The main disadvantages of this approach are the large amount of memory needed for a good resolution of the solution and the numerical problems arising when $\dot{q}(x)$ is small. To overcome these problems we developed a numerical scheme based on a pseudospectral algorithm which allows for rather accurate results for all temperatures with a reasonable amount of memory. Moreover, the use of pseudospectral methods makes the whole code rather fast.

We stress that, while the methods we are going to discuss are applied here to the Sherrington-Kirkpatrick model, they have a wider range of application. In principle they can be applied to any model with an ∞-replica symmetry breaking type solution [3].

We find that for the Sherrington-Kirkpatrick model the Parisi solution $q(x)$ is not an odd function as one might expect from its physical meaning. At any $T < T_c$, the Taylor expansion of $q(x)$ in powers of x contains both odd as well as even powers of x. The only term that is missing is x^2. The presence of the fourth order derivative was first noted by Temesvari [14]. Often, instead of $q(x)$, it is more useful to consider the overlap probability distribution function $P(q)$, which gives the probability of finding two states with mutual overlap q according to the Gibbs measure. The two quantities are related by [15,16]

$$P(q) = \frac{dx}{dq}, \tag{1}$$

where $x(q)$ is the inverse function of $q(x)$. In the absence of external magnetic fields the function $P(q)$ must be an even function of q. The computed function $q(x)$, however, is defined only for positive values; therefore it determines only the right branch of the function $P(q)$. If we define $\tilde{P}(q) = dx/dq$ for $q > 0$ then the full $P(q)$ is given by the symmetrized expression

$$P(q) = \frac{1}{2}\tilde{P}(-q) + \frac{1}{2}\tilde{P}(q). \tag{2}$$

*Electronic address: andrea.crisanti@phys.uniroma1.it

It is easy to see that the presence of nonzero even derivatives of $q(x)$ at $x=0$ makes the function $P(q)$ nonanalytical at $q=0$:

$$P(q)=c_0+c_2q^2+c_3|q|^3+\cdots, \tag{3}$$

so that $P(q)$ has discontinuous derivatives at $q=0$.

We shall discuss two different methods of computing the expansions. The first, discussed in Sec. II, performs expansion before imposing stationarity of the free energy functional. The two steps, however, can be inverted, i.e., the expansion can be done after stationarity is imposed, Sec. II. The two approaches are obviously equivalent and the advantage of using one or the other depends only on which quantity one is interested in. Since the expansions are likely to be asymptotic some resummation scheme, such as the Padé scheme discussed in Sec. IV, is needed. Finally, in Sec. V we present an integration procedure and compare the analytical results with those obtained from a direct numerical solution of the ∞-replica symmetry breaking equations.

II. EXPANSION OF THE FREE ENERGY FUNCTIONAL

The Parisi free energy f for the SK model in an external field h at temperature T is [17]

$$-f=\frac{\beta}{4}\left(1-2\,q(1)+\int_0^1 dx\,q^2(x)\right)+\int_{-\infty}^{+\infty}\frac{dy}{\sqrt{2\pi q(0)}}\exp\left(-\frac{(y-h)^2}{2\,q(0)}\right)\phi(0,y), \tag{4}$$

where $\phi(0,y)$ is the solution evaluated at $x=0$ of the Parisi equation

$$\dot{\phi}(x,y)=-\frac{\dot{q}(x)}{2}[\phi''(x,y)+\beta\,x\,\phi'(x,y)^2] \tag{5}$$

with the boundary condition

$$\phi(1,y)=\beta^{-1}\ln(2\cosh\beta y), \tag{6}$$

where we have used the standard notation and denote derivatives with respect to x by an overdot and derivatives with respect to y by a prime. The order parameter $q(x)$ at temperature T is obtained by the stationarity condition of Eq. (4) with respect to variations of $q(x)$, while the value of Eq. (4) at the stationarity point gives the free energy $f(T)$.

To expand the free energy functional (4) in powers of $\tau=T_c-T=1-T$ we observe that in the absence of external fields $q(x)$ is different from $q(1)$ only in a region $[0,x_{\max}]$ with $x_{\max}=O(\tau)$ [7], so that an expansion in powers of τ must correspond to an expansion of the same order in x. Therefore, to compute the free energy to order n, we insert into Eq. (4) the following expansions:

$$q(1)=\sum_{i=1}^{n-2}a_i\tau^i \tag{7}$$

and

$$x(q)=\sum_{i=1}^{n-3}\sum_{j=0}^{n-3-i}b_{ij}q^i\tau^j. \tag{8}$$

The coefficients of the expansion of the function $\phi(q,y)$ about $q=q(1)$ and $y=0$ can be obtained by repeated differentiation with respect to q of the equation

$$\frac{\partial\phi}{\partial q}=-\frac{1}{2}\left[\frac{\partial^2\phi}{\partial y^2}+x(q)\left(\frac{\partial\phi}{\partial y}\right)^2\right]. \tag{9}$$

Differentiating this equation j times with respect to y, mixed derivatives $\phi^{(1,j)}(q,y)$ can be eliminated in favor of derivatives with respect to y only. In the absence of an external magnetic field the last term in Eq. (4) reduces to $\phi(0,0)$, greatly simplifying the calculation since at each step we can eliminate all terms containing odd derivatives of ϕ with respect to y, such as, for example, $(\partial\phi/\partial y)^2$ in the previous equation, since all these vanish if evaluated at $y=0$, $\phi(q,y)$ being an even function of y.

Collecting all terms with the same power of τ the free energy functional (4) is written as

$$f=\sum_{i=0}^{n}c_i[\{a\},\{b\}]\tau^i. \tag{10}$$

This expression must be stationary with respect to variations of the a's and b's for any τ. Imposing stationarity of each c_i we can find the values of the parameters a and b. For example, to order τ^6 we have

$$q(x)=\left(\frac{1}{2}+\frac{3}{2}\tau+2\tau^3-9\tau^4+\frac{336}{5}\tau^5\right)x+\left(-\frac{1}{8}+\frac{25}{8}\tau+3\tau^2+38\tau^3\right)x^3+(-1-9\tau-30\tau^2)x^4+\left(\frac{351}{320}+\frac{9189}{320}\tau\right)x^5-\frac{27}{5}x^6 \tag{11}$$

and

$$x_{\max}=2\tau-4\tau^2+12\tau^3-69\tau^4+\frac{2493}{5}\tau^5-\frac{20544}{5}\tau^6. \tag{12}$$

By using this procedure we have obtained the free energy up to order 30, $q(x)$ to order 13, and $q(1)$ to order 14, because, despite the fact that the free energy is evaluated to order n, the variational relations allow one to determine $x(q)$ only to order $[(n-3)/2]$ and $q(1)$ only to order $[(n-1)/2]$.

From Eq. (11) we clearly see that $q(x)$ contains even powers of x, with the exclusion of x^2. In the next section we shall derive exact relations among the derivatives of $q(x)$ at $x=0$ from which it follows that $q^{(2)}(x=0)=0$ but $q^{(4)}(x=0)\neq 0$.

III. EXPANSION OF THE ORDER PARAMETER $q(x)$

To evaluate the derivatives of the order parameter $q(x)$ at $x=0$ we use a variational approach developed by Sommers and Dupont [11]. This method has also the advantage of leading to exact relations among derivatives of different order, so it can be used to test the findings of the previous section in a nonperturbative way. The starting point is the variational form of the Parisi free energy f:

$$-f=\frac{\beta}{4}\left(1-2\,q(1)+\int_0^1 dx\,q^2(x)\right)+\int_{-\infty}^{+\infty}\frac{dy}{\sqrt{2\pi q(0)}}\exp\left(-\frac{(y-h)^2}{2\,q(0)}\right)\phi(0,y)-\int_{-\infty}^{+\infty}dy\,P(1,y)[\phi(1,y)-T\ln(2\cosh\beta y)]$$
$$+\int_0^1 dx\int_{-\infty}^{+\infty}dy\,P(x,y)\left[\dot{\phi}(x,y)+\frac{\dot{q}(x)}{2}[\phi''(x,y)+\beta\,x\,\phi'(x,y)^2]\right]. \tag{13}$$

Imposing stationarity with respect to variations of $P(x,y)$, $P(1,y)$, $\phi(x,y)$, $\phi(0,y)$, and $q(x)$, one obtains the variational equations

$$q(x)=\int dy\,P(x,y)m^2(x,y), \tag{14}$$

$$\dot{m}(x,y)=-\frac{\dot{q}(x)}{2}[m''(x,y)+2\beta x m(x,y)m'(x,y)], \tag{15}$$

$$\dot{P}(x,y)=\frac{\dot{q}(x)}{2}[P''(x,y)-2\beta x[m(x,y)P(x,y)]'], \tag{16}$$

with initial conditions (in the absence of a magnetic field)

$$m(1,y)=\tanh(y/T), \tag{17}$$

$$P(0,y)=\delta(y). \tag{18}$$

These equations are the starting point of both the expansion discussed in this section and the numerical solution.

A time scale τ_x can be associated with the order parameter $q(x)$ such that for times of order τ_x states with an overlap equal to or greater than $q(x)$ can be reached by the system. In this picture $P(x,y)$ and $m(x,y)$ become, respectively, the probability distribution of frozen local fields y and the local magnetization in a local field y at the time scale labeled by x [1,11].

The derivatives of $q(x)$ can be obtained by successive x derivation of Eq. (14). The procedure is simplified by the use of the following identity [9]:

$$\frac{d}{dx}\int dy\,P(x,y)\,f(x,y)=\int dy\,P(x,y)\Omega(x,y)f(x,y) \tag{19}$$

where

$$\Omega(x,y)=\frac{\partial}{\partial x}+\frac{\dot{q}}{2}\left(\frac{\partial^2}{\partial y^2}+2\,\beta\,x\,m(x,y)\frac{\partial}{\partial y}\right). \tag{20}$$

The application of the operator $\Omega(x,y)$ generates derivatives of the function $m(x,y)$ with respect to x and y. Mixed derivatives such as $m^{(1,j)}(x,y)$ can be eliminated in favor of derivatives of $m(x,y)$ with respect only to y by deriving Eq. (15) j times with respect to y.

The first application of this procedure yields

$$\dot{q}(x)=\dot{q}(x)\int dy\,P(x,y)(m')^2 \tag{21}$$

which for $\dot{q}(x)\neq 0$ simply reads

$$1=\int dy\,P(x,y)\,m'(x,y)^2. \tag{22}$$

The procedure can be iterated infinitely. For example, the next three applications lead respectively to

$$0=-\frac{2x}{T}\int dy\,P(m')^3+\int dy\,P(m'')^2, \tag{23}$$

$$\frac{2}{T}\int dy\,P(m')^3=\dot{q}\int P\,dy\left[(m''')^2-\frac{12x}{T}m'(m'')^2+6\left(\frac{x}{T}\right)^2(m')^4\right], \tag{24}$$

and

$$\int P\,dy\left(\frac{(18x\dot{q}+6x^2\ddot{q})(m')^4}{T^2}-\frac{(18\dot{q}T+12x\ddot{q}T-120m'x^2\dot{q}^2)m'(m'')^2}{T^2}+\frac{-30x\dot{q}^2(m'')^2+\ddot{q}m'''T-20x\dot{q}^2m'(m''')}{T}m'''-\frac{24x^3\dot{q}^2(m')^5}{T^3}+\dot{q}^2(m'''')^2\right)=0. \tag{25}$$

We are interested in the derivatives of $q(x)$ at $x=0$, so we take the limit $x\to 0$ of the above equations. The limit can be done in a trivial way and, since the function $P(0,y)$ reduces to a δ function [see Eq. (18)], the equations are greatly simplified. Moreover, since $m(x,y)$ is an odd function of y for any x, clearly $m^{(0,j)}(0,0)=0$ for any even j. In this limit Eqs. (22), (24), and (25) reduce, respectively, to

$$1=m'(0,0), \tag{26}$$

$$\frac{2}{T}m'(0,0)^3=\dot{q}(0)m'''(0,0)^2, \tag{27}$$

$$\ddot{q}(0)m'''(0,0)^2=0, \tag{28}$$

while Eqs. (14) and (23) become trivial identities.

From Eqs. (26) and (27) we have

$$m'''(0,0)=-\sqrt{\frac{2}{T\dot{q}(0)}}\neq 0; \tag{29}$$

therefore Eq. (28) implies that $\ddot{q}(0)=0$, as already found in Ref. [9].

To obtain information on the fourth derivative of $q(x)$ the above procedure must be iterated twice more. Since successive derivatives yield expressions with a rapidly growing number of terms we only report the result for the limit $x\to 0$:

$$\frac{18\dot{q}(0)}{T^2}+q^{(3)}(0)m'''(0,0)^2-\frac{38\dot{q}(0)^2m'''(0,0)^2}{T}$$

$$+\dot{q}(0)^3m^{(0,5)}(0,0)=0, \tag{30}$$

$$q^{(4)}(0)m'''(0,0)-\frac{96\dot{q}(0)m'''(0,0)^3}{T}=0, \tag{31}$$

where Eq. (26) and the exact result $\ddot{q}(0)=0$ have been used. Note that Eq. (31), with Eq. (29), gives a complete determination of the quartic derivative of $q(x)$ at $x=0$ as a function of the temperature T and of the first derivative $\dot{q}(x=0)$:

$$q^{(4)}(0)=-\frac{96\sqrt{2}\dot{q}(0)^{5/2}}{T^{3/2}}. \tag{32}$$

This relation shows that the function $q(x)$ does not have a well defined parity [14].

Going to higher orders one can show that all the even derivatives can be expressed in terms of the odd ones; for instance, we have

$$q^{(6)}(0)=-\frac{34272\sqrt{2}\dot{q}(0)^{7/2}}{T^{5/2}}-\frac{1056\sqrt{2}\dot{q}(0)^{3/2}q^{(3)}(0)}{T^{3/2}}, \tag{33}$$

and so on.

In the limit $T\to 0$ we have $T\dot{q}(0)=0.743\pm 0.002$. Note that if we take $\dot{q}(0)\sim 1/T$ for $T\to 0$ the previous equation implies that all the derivatives diverge with the temperature as $q^{(n)}(0)\sim 1/T^n$, in agreement with the Parisi-Toulouse scaling $q(x,T)=q(\beta x)$ [10,18]. Note that we have derived this scaling under the strong hypothesis that it must be valid asymptotically for $T\to 0$ and $\beta x\to 0$.

This approach also provides an alternative method to compute the expansion of $q(x)$ in powers of x and τ: starting from $q(x)$ evaluated at a given order in x and τ we can compute $m^{(0,j)}(0,0)$ through Eq. (15) and then $q(x)$ at the next order through the set of Eqs. (26), (28), (30), (31), and so on. The set of equations can be solved iteratively. By this method we were able to compute the series expansion of $q(x)$ up to order 20, improving the results of the previous section.

IV. RESUMMATION OF THE EXPANSIONS

Unfortunately all the expansions derived in the previous sections are likely to be asymptotic and to obtain sensible estimates of the various quantities of interest some form of resummation must be done. Here we shall consider the standard Padé approximant which for a series of degree $N+M$ reads [19]

$$P_M^N(x)=\frac{\sum_{i=0}^{N}a_ix^i}{1+\sum_{i=1}^{M}b_ix^i}, \tag{34}$$

where the coefficients are chosen so that the first $(N+M+1)$ terms of the Taylor expansion of $P_M^N(x)$ match the first $(N+M+1)$ terms of the original series. In the following we shall call this the Padé approximant (N,M).

The first problem we face is that, despite the fact that the series have alternate signs, they are not Stijlties integral and therefore we cannot obtain in a systematic way a sequence of lower and upper bounds [19]. This difficulty can be overcome by noticing that most of the quantities we are interested in, such as, for example, free energy or entropy or $q(1)$, do have a null derivative at $T=0$. Therefore an indication of the quality of the approximants can be obtained by analyzing the behavior near $T=0$. For example, the free energy as a function of T is reproduced quite well by many Padé approximants, even at very low orders; however, some of these have a positive derivative at $T=0$ while others have a negative one (see Fig. 1). By inspecting the figure we can safely assume that approximants with positive derivatives give an upper bound, and those with negative derivatives a lower bound, for the true free energy [20].

As a general fact we obtain the result that the best Padé approximants at a given order in τ are those with nearly the same degree in the numerator and the denominator. We stress, however, that as usual with asymptotic expansion an increase of the order in τ does not necessarily correspond to an improvement of the precision. With this procedure we obtain for the free energy an estimate with at least 16 digits

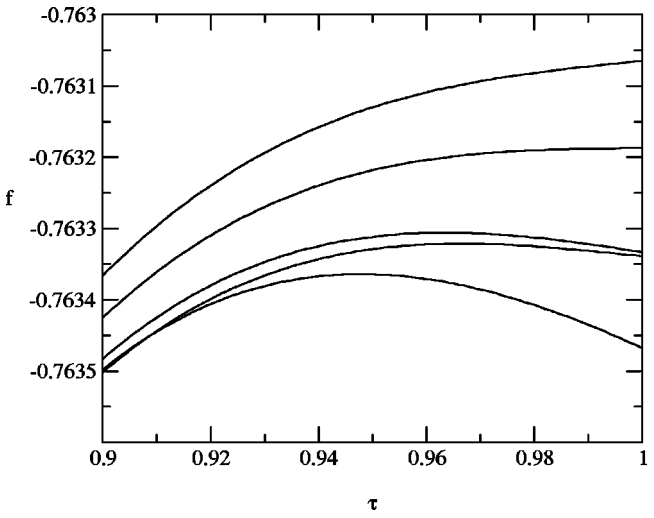

FIG. 1. Free energy as a function of $\tau=1-T$ for different Padé approximants. Top to bottom: (14,16), (13,12), (12,11), (10,11), and (17,10).

precision at $T=0.9$ and eight digits at $T=0.5$, and for the ground state energy $E_0=-0.763\,21\pm0.000\,03$, in agreement with Parisi's estimate $E_0=-0.7633\pm0.0001$ [17]. A similar analysis can be used to determine the value of $x_{\max}$ as a function of temperature; the result is shown in Fig. 2. The value of the breaking point is finite in the limit $T\to0$,

$$x_{\max}(0)=0.548\pm0.005 \tag{35}$$

(see the inset of Fig. 2), and slightly larger than the value 1/2 predicted by the Parisi-Toulouse scaling, in agreement with the approximate nature of this relation [10,18].

The analysis of the function $q(x,T)$ is more complex, because not only is the Taylor expansion of $q(x)$ in powers of x around any $0<x<x_{\max}$ likely to be asymptotic for any fixed temperature, but the expansion in τ of the coefficients of the x expansion is itself nonconvergent. Therefore one should use a double Padé expansion, one for the coefficients

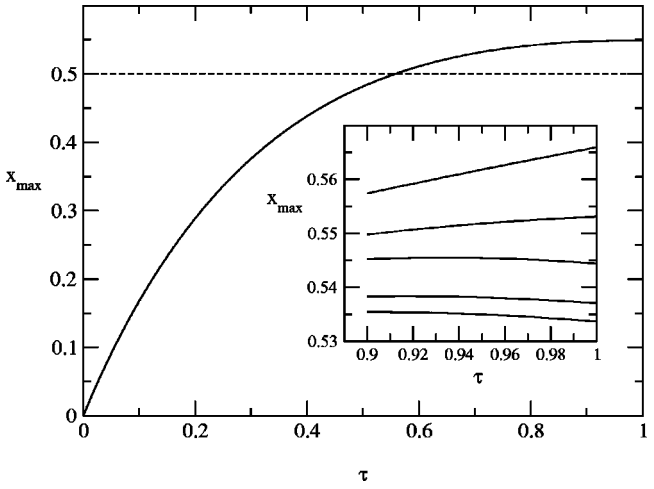

FIG. 2. $x_{\max}$ as a function of $\tau=1-T$. Inset: $x_{\max}$ as a function of $\tau=1-T$ with different Padé approximants. From top to bottom: (7,10), (9,9), (8,12), (6,7), and (7,8).

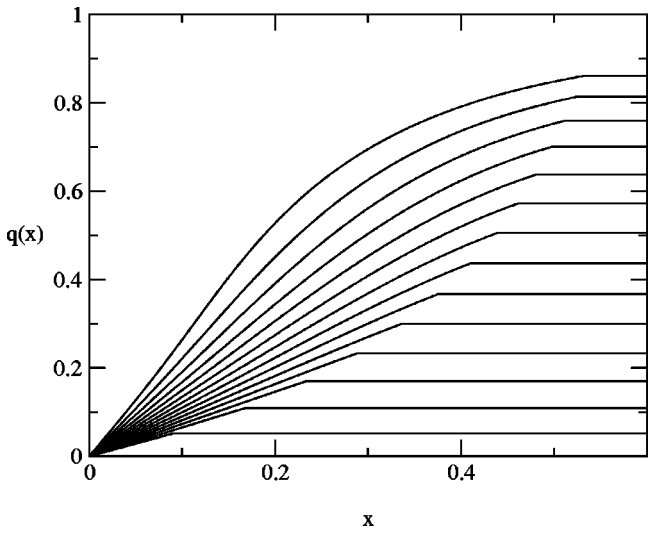

FIG. 3. $q(x)$ as a function of x for various temperatures. From bottom to top: $T=0.95$ to $T=0.30$ in steps of 0.05.

and one for $q(x)$. The procedure, however, is quite difficult because we do not have a systematic way of choosing the best approximant and, moreover, coefficients of higher order are known with less precision in τ. A better approach is to construct the function $q(x)$ directly point by point by computing $q(mx_{\max})$ where $m=i/n$ $(i=0,1,\ldots,n)$ for fixed n. For any m and T the quantity $q(mx_{\max})$ is itself a power series in τ which can be summed up using Padé approximants. With this procedure the function $q(x)$ can be determined for different x resolution just by changing the value of n, e.g., $n=50,100,1000$, and using the value of $x_{\max}$ previously found (see Fig. 2). In Fig. 3 the function $q(x)$ is shown for various temperatures T.

This method can be extended to any function of x or q; for example, we computed the overlap probability function $P(mq_{\max})$ in a wide range of temperature $T>0.3$ (see Fig. 4). We found that the best Padé approximant is given by (12,7). By using the relation (1) we can have an independent estimation of $q(x)$ with which to test the precision of our results. By using a norm $d_\infty(q,q')=\max_{0\leqslant x\leqslant1}|q(x)-q'(x)|$ and expansions up to order 20 we find, for example, that $d_\infty(q,q')=O(10^{-5})$ for $T=0.6$ and $d_\infty(q,q')=O(10^{-4})$ for $T=0.4$.

The form of the function $q(x)$ confirms the prediction of Ref. [10] obtained from interpolation of the 11-RSB solution. In particular, it confirms the approximate scaling $q(x,T)\sim q(x/T)$ at low temperatures (see Fig. 5). Note that the scaling fails when $\beta x\sim O(1)$, in agreement with the findings of the previous section.

Finally, we mention that an alternative resummation technique based on the Borel transform gives results consistent with those obtained with the Padé approximants.

V. NUMERICAL INTEGRATION OF THE ∞-RSB EQUATIONS

To check the analytical results of the previous sections we have solved the ∞-RSB equations (14)–(18) numerically on

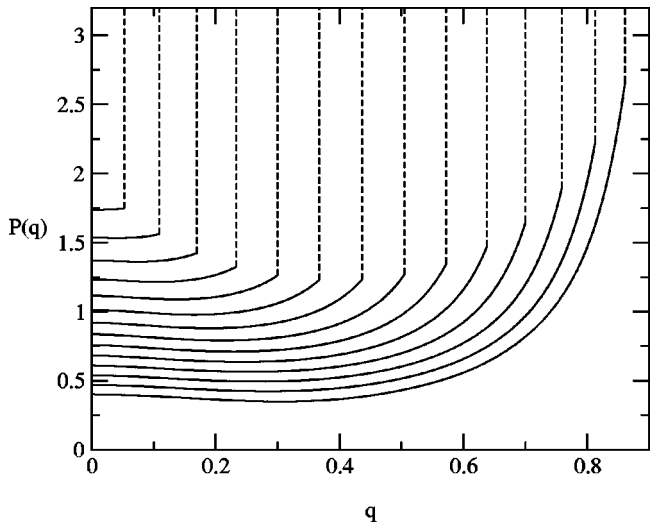

FIG. 4. $P(q)$ as a function of q for various temperatures. From left to right: $T=0.95$ to $T=0.30$ in steps of 0.05. The data were obtained with a (12,7) approximant. Note that $P(q)$ attains its minimum value for $q>0$. This happens for any temperature $T<0.961\,938\ldots$.

a discrete set of points in the infinite strip $[0\leqslant x\leqslant 1;\ -\infty<y<\infty]$ and determined $q(x)$, $P(x,y)$, and $m(x,y)$. The numerical method is based on the iterative procedure of Ref. [12]: from an initial guess of $q(x)$ the fields $m(x,y)$ and $P(x,y)$ and the associated $q(x)$ are computed in order as follows.

(i) Compute $m(x,y)$ by integrating Eqs. (15) from $x=x_0$ to $x=0$ with initial condition (17).

(ii) Compute $P(x,y)$ by integrating Eqs. (16) from $x=0$ to $x=x_0$ with initial condition (18).

(iii) Compute $q(x)$ using Eq. (14).

Here $x_0\leqslant 1$ (see later). The steps $1\rightarrow 2\rightarrow 3$ are repeated until a reasonable convergence is reached, typically a mean square error on q, P, and m of the order of $O(10^{-6})$.

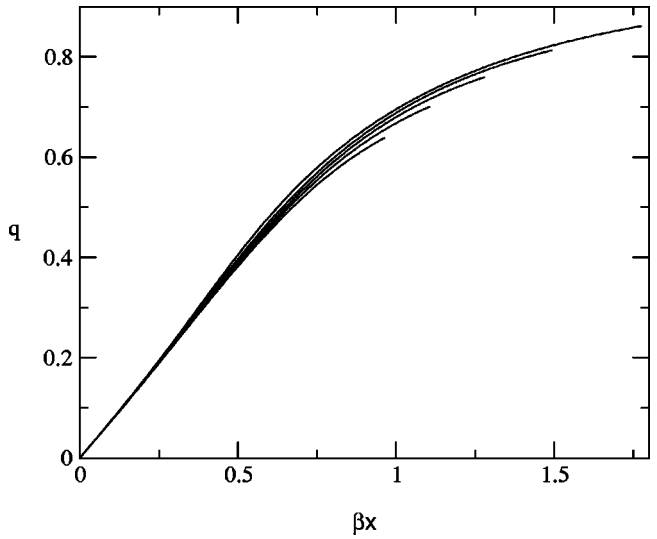

FIG. 5. q as a function of βx for different values of T. Top to bottom: $T=0.30$, $T=0.35$, $T=0.40$, $T=0.45$, and $T=0.50$.

The core of the numerical scheme is the integration of the partial differential equations (15) and (16) along the x direction which, in contrast to previous numerical studies [12,13], is done in the Fourier space of the y variables, where the equations take the form

$$\frac{\partial}{\partial x}m(x,k)=\frac{k^2\dot{q}(x)}{2}m(x,k)-\frac{\beta\dot{q}(x)}{2}ik\mathcal{FT}[m^2](x,k) \tag{36}$$

and

$$\frac{\partial}{\partial x}P(x,k)=-\frac{k^2\dot{q}(x)}{2}P(x,k)-\beta\dot{q}(x)ik\mathcal{FT}[P\,m](x,k). \tag{37}$$

For each wave vector k these are ordinary differential equations which can be integrated using standard methods. To avoid the time consuming calculation of the convolutions in the nonlinear term we use a pseudospectral [21] code on a grid mesh of $N_x\times N_y$ points, which covers the x interval $[0,x_0]$ and the y interval $[-y_{\max},y_{\max}]$. The truncation of the wave number may introduce anisotropic effects for large k; therefore to ensure a better isotropy of the numerical treatment we perform dealiasing via an $N_y/2$ truncation [22]. Finally, the x integration was performed using a third order Adam-Bashfort scheme which has the advantage of reducing the number of fast Fourier calls [23]. Typical values used are $N_x=100$–5000, $N_y=512$–4096, and $y_{\max}=12$–48. The difference between the values used for N_x and N_y follows from the observation that, if the solution in the y direction is smooth enough, then only a few low wave vectors are excited. The value of the parameter $y_{\max}$ fixes the y range where the solution is assumed different from zero, since in the numerical algorithm it is implicitly assumed that

$$P(x,y)\equiv m(x,y)=0,\quad |y|>y_{\max}. \tag{38}$$

This explains the rather large value used. The number of iterations necessary to reach a mean square error on q, P, and m of order $O(10^{-6})$ depends on the initial guess of $q(x)$ but it is typically a few hundred.

In Fig. 6 are shown the order parameter $q(x)$ and the overlap probability distribution function $P(q)$ at $T=0.6$ computed for increasing x resolution and $x_0=1$. As expected the agreement between the numerical and the perturbative solutions increases with the number N_x of x grid points. However, the convergence is not uniform: it is rather fast far from $x_{\max}$ and much slower for $x\simeq x_{\max}$ [see the inset of Fig. 6(a)]. This is not unexpected because for $x=x_{\max}$ the derivative of the order parameter $q^{(1)}(x)$ has a cusp:

$$\lim_{x\rightarrow x_{\max}^-}q^{(1)}(x)>0,\qquad \lim_{x\rightarrow x_{\max}^+}q^{(1)}(x)=0, \tag{39}$$

making convergence more difficult. We recall that in deriving Eqs. (15) and (16) differentiability of $q(x)$ was assumed.

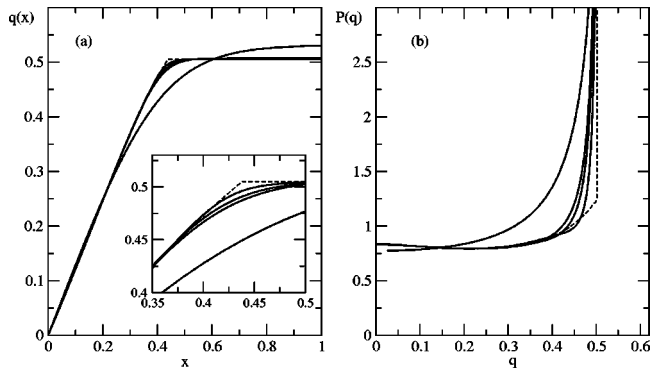

FIG. 6. $q(x)$ as a function of x (a) and $P(q)$ as a function of x (b) at $T=0.6$ for [(a) bottom to top; (b) left to right] $N_x=50$, $N_x=500$, $N_x=1000$, and $N_x=5000$. In all cases $x_0=1$, $y_{\max}=48$, and $N_y=4096$. The dashed line is the result from the perturbative solution discussed in the previous sections. Inset in (a) enlargement of the region near $x_{\max}$.

The use of lower order integration schemes, such as second order Adam-Bashfort or Euler schemes, does not give measurable improvements.

Larger values of N_x require more computer memory; therefore to increase the precision we adopted a different approach. Since $\dot{q}(x)=0$ for $x>x_{\max}$ Eqs. (15) and (16) are trivial in this range and we can reduce the upper bound of the x integration from $x=1$ to $x=x_0=x_{\max}$. This obviously requires a knowledge of $x_{\max}$ for the given temperature. However, if we assume no *a priori* knowledge of $x_{\max}$ we must proceed with successive approximations: we start from $x_0=1$ and then reduce it until we "hit" the value of $x_{\max}$. This procedure is simplified by the fact that if $x_0<x_{\max}$ the shape of $q(x)$ near x_0 changes dramatically, with the concavity passing from negative values for $x_0>x_{\max}$ to positive values for $x_0<x_{\max}$. In Fig. 7 are shown $q(x)$ (a) and $P(q)$ (b) at $T=0.6$ for different values of x_0; the improvement is rather evident. As an additional check we have considered the equality

$$1-\int_0^1 dx\, q(x)=T, \tag{40}$$

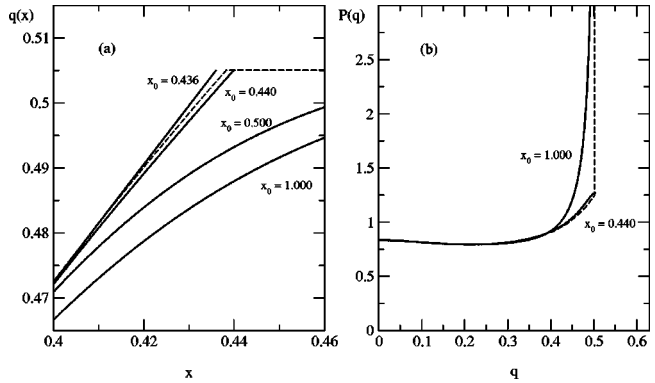

FIG. 7. (a) $q(x)$ for $T=0.6$ near $x_{\max}$ for different x_0. (b) $P(q)$ for $T=0.6$ for different x_0. In all cases $N_x=500$, $y_{\max}=48$, and $N_y=4096$. The dashed line is the result from the perturbative solution discussed in the previous sections.

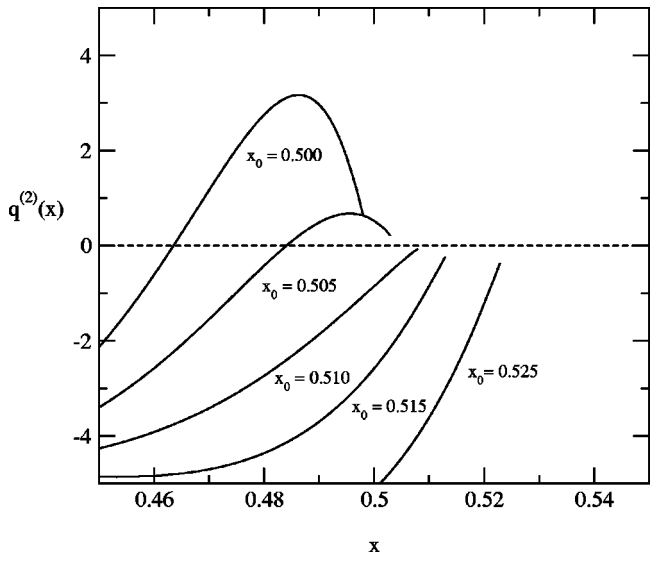

FIG. 8. Second derivative of $q(x)$ for $T=0.4$ for different x_0 and $N_x=500$, $y_{\max}=48$, and $N_y=4096$.

which is satisfied by our numerical solution for all studied temperatures with at least four digits. For example, for $T=0.8$ we get $0.799\,99(4)$, while for $T=0.5$ the value is $0.499\,99(3)$.

Note that by fine tuning x_0 not only can we have a good solution for $q(x)$ at the given temperature, but we also have *the value* of x_0. This is best seen by analyzing the concavity of $q(x)$ near x_0. In Fig. 8 we show the second derivative of $q(x)$ near x_0 for $T=0.4$ and $N_x=500$, from which one may conclude that $0.505<x_{\max}<0.510$.

A careful analysis of the stability of this result as a function of N_x (see Fig. 9), reveals, however, that the correct estimation is $0.510<x_{\max}<0.515$, in rather good agreement with the analytical result $x_{\max}=0.5111\pm0.0002$. The same analysis for $T=0.6$ leads to $0.438<x_{\max}<0.440$.

We are now in a position to check the results of the previous section about the derivative of the order parameter at $x=0$, and in particular the conclusion

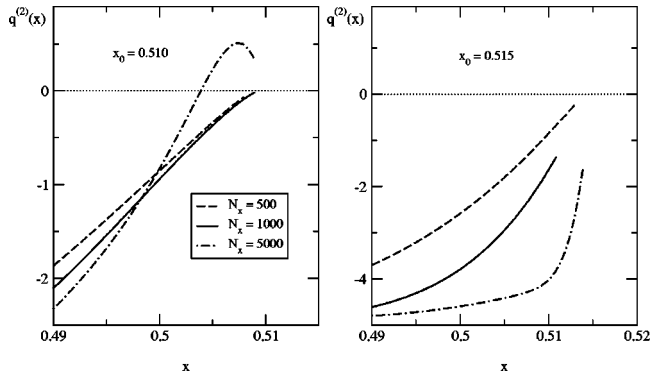

FIG. 9. Second derivative of $q(x)$ for $T=0.4$ for different N_x and $x_0=0.510$, $y_{\max}=48$, and $N_y=4096$. Left panel: $x_0=0.510$; increasing N_x leads to a positive value of $q^{(2)}(x_0)$ implying $x_0=0.510<x_{\max}$. Right panel: $x_0=0.515$; increasing N_x leads to a more negative value of $q^{(2)}(x_0)$ implying $x_0=0.515>x_{\max}$.

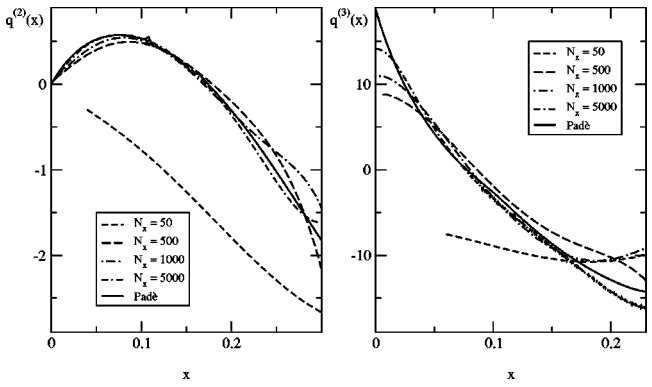

FIG. 10. Left panel: second derivative of $q(x)$ at $T=0.6$ and different N_x. Right panel: third derivative of $q(x)$ at $T=0.6$ and different N_x. In both cases $x_0=1$, $y_{\max}=48$, and $N_y=4096$. The full line is the perturbative result.

$$\lim_{x\to 0} q^{(3)}(x) > 0. \tag{41}$$

In Fig. 10 we show the second and third derivatives of $q(x)$ obtained from numerical differentiation of $q(x)$. The agreement with the perturbative result is sufficiently good; moreover, from the right panel of Fig. 10 we clearly see that the prediction (41) is verified.

We conclude this section with a short discussion of the entropy which, using the stationarity of the free energy functional (13), can be written as

$$s = -\frac{\beta^2}{4}[1-q(1)]^2 + \int_{-\infty}^{\infty} dy\, P(1,y)[\ln 2\cosh\beta y - y\tanh(\beta y)]. \tag{42}$$

For other equivalent forms see, e.g., Ref. [3]. The entropy as a function of temperature is shown in the left panel of Fig. 11. The entropy must vanish quadratically with the temperature as $T\to 0$ [11]. From our numerical data we find

$$\lim_{T\to 0}\frac{s(T)}{T^2} = a \simeq 0.72 \tag{43}$$

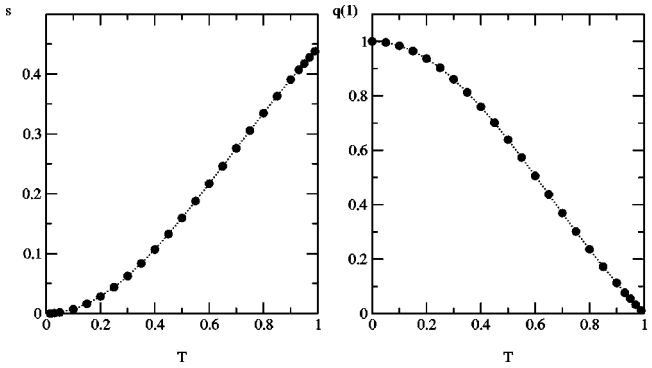

FIG. 11. Left panel: entropy s as a function of temperature T. Right panel: $q(1)$ as a function of temperature T.

to be compared with 0.718 ± 0.004 of the analytic expansions.

In the limit $T\to 0$ the quantity $1-q(1)$ must also vanish as T^2 [11]. The behavior of $q(1)$ as a function of T is shown in the right panel of Fig. 11. Using these data we obtain

$$\lim_{T\to 0}\frac{1-q(1)}{T^2} \simeq 1.60, \tag{44}$$

in very good agreement with the value 1.60 ± 0.01 obtained with the expansions of the previous sections.

VI. CONCLUSIONS

In this paper we have studied the properties of the ∞-replica symmetry breaking solution of the Sherrington-Kirkpatrick model without external fields. Using high order expansions in $\tau = T_c - T$ we are able to compute the order parameter $q(x)$ and other relevant quantities for a large range of temperatures with high precision. In particular, we found that $q(x)$ *is not* an odd function of x, confirming the prediction of Ref. [14]. A direct consequence of this is that the overlap probability distribution function $P(q)$ has discontinuous derivatives at $q=0$. Another consequence of our findings is that the Parisi-Toulouse scaling becomes exact asymptotically for $T\to 0$ *and* $\beta x\to 0$, while for $T\to 0$ it is a fairly good approximation. This is also consistent with the $T=0$ limit of the breaking point which we found to be $x_{\max}(0)=0.548\pm 0.005$.

Having reached very high orders we can reasonably speculate on the analytical properties of the function $q(x)$. In particular, we believe that all the expansions in powers of τ are asymptotic expansions; and at any temperature, the function $q(x)$ is infinitely differentiable but not analytical for any x; in particular, the Taylor expansion of the function $q(x)$ around any $0<x<x_{\max}$ does not converge but is asymptotic.

This singular behavior is not connected either with the replica limit or with the Parisi ansatz; it actually originates from the singularities in the complex plain of the initial condition of the Parisi equation: $f(1,y)=\ln 2\cosh\beta y$. This is clearly seen for the replica symmetric solution

$$q = \int_{-\infty}^{+\infty}\frac{dz}{\sqrt{2\pi}} e^{-2z^2/2}\tanh^2(\beta\sqrt{q}z).$$

In this case it is easy to prove that the expansion of $(1-T^2)$ in powers of $p=\beta^2 q$ is asymptotic because it corresponds to substituting $\tanh^2 z$ in the integrand with its Taylor expansion, which is not convergent on the whole real axes. Then one can prove that the expansion of q in powers of $\tau = 1-T$ is asymptotic, recalling that standard manipulation (e.g., multiplication, division, inversion, etc.) on an asymptotic expansion in a power series does not change its character. A detailed treatment of the RSB solution is much more complex, but the origin of the asymptotic character is likely to be the same. Indeed, an expansion in small τ (and therefore in small q) corresponds to an expansion in small y of all the quantities like $f(x,y)$ and $m(x,y)$; the appearance

of integrals of the form $\int P f\, dy$ where $P(x,y) \sim \exp(-y^2/x)$ generates asymptotic expansions since the Taylor expansions of $f(x,y)$ and $m(x,y)$ in powers of y do not converge on the whole real axes. These arguments can be very useful in practice to guess the position of the singularities of the Borel transform if one wants to sum the expansions through a conformal mapping [24]. For instance, in the expression of the free energy integrals of the following form appear:

$$\int_{-\infty}^{+\infty} \frac{dz}{\sqrt{2\pi\tau}} e^{-z^2/2\tau} \ln\cosh(z). \tag{45}$$

The singularities of the Borel transform of the previous integral are located on a cut running from $-\infty$ to $-\pi^2/8$ and a possible guess is that this is also the singularity structure of the Borel transform of the free energy. This guess is supported by analysis of the series expansions.

The analytical results have been compared with numerical solutions of the ∞-replica symmetry breaking equations. We have developed a numerical approach based on a pseudospectral code which leads to strong enhancement of the quality of the numerical results. We have also shown how, for example, to determine the value of $x_{\max}$ numerically. In all cases the agreement between the numerical and the analytical results is rather good.

We conclude by stressing that our results go beyond the interest in the Sherrington-Kirkpatrick model, since the method we used here is far more general and can be employed in a wider class of models with generalized ∞-replica symmetry breaking equations, such as those introduced in Ref. [3]. In particular, in this reference the numerical method was applied to an optimization problem (3-SAT) model, and the extension to other relevant models is under development.

A.C. acknowledges support from the INFM-SMC.

[1] M. Mezard, G. Parisi, and M. Virasoro, *Spin Glass Theory and Beyond* (World Scientific, Singapore, 1987).
[2] K.H. Fischer and J.A. Hertz, *Spin-Glasses* (Cambridge University Press, Cambridge, England, 1991).
[3] A. Crisanti, L. Leuzzi, and G. Parisi, J. Phys. A **35**, 481 (2002).
[4] E. Gardner, Nucl. Phys. B **257**, 747 (1985).
[5] T.R. Kirkpatrick and D. Thirumalai, Phys. Rev. B **36**, 5388 (1987).
[6] M. Sellitto, M. Nicodemi, and J.J. Arenzon, J. Phys. I **7**, 945 (1997).
[7] G. Parisi, Phys. Rev. Lett. **43**, 1754 (1979); J. Phys. A **13**, L115 (1980).
[8] I. Kondor, J. Phys. A **16**, L127 (1983).
[9] H.-J. Sommers, J. Phys. (France) Lett. **46**, L-779 (1985).
[10] J. Vannimenus, G. Toulouse, and G. Parisi, J. Phys. (France) **42**, 565 (1981).
[11] H.J. Sommers and W. Dupont, J. Phys. C **17**, 5785 (1984).
[12] K. Nemoto, J. Phys. C **20**, 1325 (1987).
[13] P. Biscari, J. Phys. A **23**, 3861 (1990).
[14] T. Temesvari, J. Phys. A **22**, L1025 (1989).
[15] C. De Dominicis and A.P. Young, J. Phys. A **16**, 2063 (1983).
[16] G. Parisi, Phys. Rev. Lett. **50**, 1946 (1983).
[17] G. Parisi, J. Phys. A **13**, L115 (1980).
[18] G. Parisi and G. Toulouse, J. Phys. (France) Lett. **41**, L-361 (1980).
[19] C.M. Bender and S.A. Orszag, *Advanced Mathematical Methods for Scientists and Engineers* (McGraw-Hill, New York, 1978).
[20] We note that it is possible to impose a null derivative at $T=0$ directly in the Padé approximants. This, however, does not produce a measurable improvement of the precision at a given order, making it at the same time more difficult to have control of the convergence.
[21] S.A. Orszag, *Studies in Applied Mathematics* (Cambridge University Press, Cambridge, England, 1971), Vol. 4, p. 293.
[22] G.S. Patterson and S.A. Orszag, Phys. Fluids **14**, 2538 (1971).
[23] See, e.g., J.H. Ferziger and M. Perić, *Computational Methods for Fluid Dynamics* (Springer-Verlag, Berlin, 1996).
[24] G. Parisi, *Statistical Field Theory* (Addison-Wesley, New York, 1988).